

This article was downloaded by:

On: 25 January 2011

Access details: *Access Details: Free Access*

Publisher *Taylor & Francis*

Informa Ltd Registered in England and Wales Registered Number: 1072954 Registered office: Mortimer House, 37-41 Mortimer Street, London W1T 3JH, UK



## Separation Science and Technology

Publication details, including instructions for authors and subscription information:

<http://www.informaworld.com/smpp/title~content=t713708471>

### A New Tangential Streaming Potential Setup for the Electrokinetic Characterization of Tubular Membranes

P. Fievet<sup>a</sup>; M. Sbaï<sup>a</sup>; A. Szymczyk<sup>a</sup>; C. Magnenet<sup>a</sup>; C. Labbez<sup>a</sup>; A. Vidonne<sup>a</sup>

<sup>a</sup> Laboratoire de Chimie des Matériaux et Interfaces, Besançon cedex, France

Online publication date: 08 July 2010

**To cite this Article** Fievet, P. , Sbaï, M. , Szymczyk, A. , Magnenet, C. , Labbez, C. and Vidonne, A.(2004) 'A New Tangential Streaming Potential Setup for the Electrokinetic Characterization of Tubular Membranes', *Separation Science and Technology*, 39: 13, 2931 — 2949

**To link to this Article:** DOI: 10.1081/SS-200028652

URL: <http://dx.doi.org/10.1081/SS-200028652>

## PLEASE SCROLL DOWN FOR ARTICLE

Full terms and conditions of use: <http://www.informaworld.com/terms-and-conditions-of-access.pdf>

This article may be used for research, teaching and private study purposes. Any substantial or systematic reproduction, re-distribution, re-selling, loan or sub-licensing, systematic supply or distribution in any form to anyone is expressly forbidden.

The publisher does not give any warranty express or implied or make any representation that the contents will be complete or accurate or up to date. The accuracy of any instructions, formulae and drug doses should be independently verified with primary sources. The publisher shall not be liable for any loss, actions, claims, proceedings, demand or costs or damages whatsoever or howsoever caused arising directly or indirectly in connection with or arising out of the use of this material.

## A New Tangential Streaming Potential Setup for the Electrokinetic Characterization of Tubular Membranes

P. Fievet,\* M. Sbaï, A. Szymczyk, C. Magnenet, C. Labbez,  
and A. Vidonne

Laboratoire de Chimie des Matériaux et Interfaces, Besançon cedex,  
France

### ABSTRACT

A new electrokinetic setup was developed for assessing the active layer  $\zeta$ -potential of tubular membranes based on tangential streaming potential and electrical resistance measurements. Although the flow was not wholly laminar (because of the large hydraulic diameter of channels), the electrokinetics theory could be used to convert the streaming potential data into  $\zeta$ -potentials because the electrical double layer lay within a laminar sublayer near the channel walls. Electrical resistance data allowed for the account of the conduction phenomenon through the membrane porous body. The new device was tested over a range of pH with a tubular ceramic membrane composed of three channels with a titania active

---

\*Correspondence: P. Fievet, Laboratoire de Chimie des Matériaux et Interfaces, 16 route de Gray, 25 030 Besançon cedex, France; Fax: +33-3-81-66-20-33; E-mail: patrick.fievet@univ-fcomte.fr.

2931

DOI: 10.1081/SS-200028652  
Copyright © 2004 by Marcel Dekker, Inc.

0149-6395 (Print); 1520-5754 (Online)  
[www.dekker.com](http://www.dekker.com)

layer. The isoelectric point was found to be in good agreement with that determined from salt retention data. The  $\zeta$ -potential value determined at pH = 3.5 using the present device was compared with that obtained on a flat membrane made of the same material using the traditional microslit electrokinetic setup. A good agreement between the two measurements was observed. It was shown that neglecting the electric conduction phenomenon through the membrane porous body leads to a low underestimation of the  $\zeta$ -potential (less than  $\sim 20\%$ ). This is related to the large size of channels. The contribution of the membrane porous body was found to be independent of the pH of solution. This suggests that the support layer of the membrane would make a decisive contribution to the electric conductivity of membrane porous body.

**Key Words:** Tangential streaming potential; Zeta potential; Turbulent flow; Electric conductance; Surface conduction; Tubular membrane.

## 1. INTRODUCTION

The zeta potential ( $\zeta$ ), defined as the electrical potential at the hydrodynamic plane of shear, is an important and reliable indicator of the membrane surface charge that interacts with its surroundings, and knowledge of it is essential for the design and operation of membrane processes. The most widely used technique for assessing this fundamental feature is the so-called streaming potential method, the streaming potential being defined as the electrical potential difference ( $\Delta\varphi_s$ ) developed in the solution flowing along the charged solid surface under a pressure difference ( $\Delta P$ ).

Streaming potential measurements can be performed in two different ways: by flow through the membrane (transmembrane streaming potential)<sup>[1-7]</sup> or by flow across the top surface of the membrane (tangential streaming potential).<sup>[7-13]</sup> The first procedure has the advantage of experimental simplicity but has the drawback not to differentiate between various layers of a multilayer membrane (like all nano- and ultrafiltration membranes are). This is important because, while a sole layer (i.e., the skin layer) rules the membrane selectivity, other layers may affect the measurement of the streaming potential.<sup>[14,15]</sup> In addition to the influence of the different structures (non-negligible pressure drop through the different layers), the selective behavior of some active layers also influences the value of the pressure-induced electrical potential difference.<sup>[16-18]</sup> In this case, the electrical potential difference measured between the membrane pore ends results from both concentration and pressure gradients and by definition is no more a streaming potential.

In such cases, tangential streaming potential measurements appear as an alternative method providing direct information about the membrane top layer

(i.e., active layer). Up to now, applied to flat membranes, the tangential technique consists of applying a pressure difference across a thin channel formed by clamping two identical flat membrane samples separated by a spacer (clamping cell). In the classical form of this method,  $\Delta P$  and  $\Delta\varphi_s$  are measured experimentally at various spacer thicknesses (e.g., heights of channel) so as to determine the correct  $\zeta$ -potential.<sup>[11,13,19]</sup> Literature shows that all clamping cells developed to measure the  $\zeta$ -potential of flat surfaces meet the hydrodynamic condition of laminar flow with a fully developed parabolic velocity distribution. In this case, conversion of tangential streaming potential data into  $\zeta$ -potential can be made from either the classical Helmholtz-Smoluchowski equation or a version of this equation including surface conductance. Recently, Yaroshchuk and Ribitsch<sup>[20]</sup> have suggested that the membrane porous body conductance may play a non-negligible role in the tangential streaming potential measurement. This was confirmed in a recent paper with a ceramic membrane made of the same material as the membrane studied in the present work by performing both tangential streaming potential and conductance measurements at various channel heights.<sup>[19]</sup>

In this paper, we present and test an electrokinetic setup for the determination of  $\zeta$ -potential of tubular membranes from tangential streaming potential measurements under conditions of turbulent flow. The study was performed with a three-channel tubular membrane close to the NF range over a range of pH. Although the flow was not wholly laminar (because of the large hydraulic diameter of channels), the Helmholtz-Smoluchowski equation could be used to convert the streaming potential data into  $\zeta$ -potentials due to the fact that the EDL lay within a laminar sublayer near the channel walls.  $\zeta$ -potentials calculated from the Helmholtz-Smoluchowski equation were compared with those determined by combining tangential streaming potential with electrical conductance measurements.

## 2. THEORY

When a liquid is forced to flow through a channel (whose walls are charged) under an applied hydrostatic pressure, the charges in the mobile part of the electrical double layer (EDL) near the wall are carried toward the low-pressure side, resulting in an electrical current in the direction of flow, called the streaming current,  $I_s$ . The accumulation of charge at one end sets up an electric field that acts to force the charges to move in the opposite direction of the streaming current. This generates an electrical current called the current conduction,  $I_c$ . When this latter equals the streaming current, a steady state is achieved ( $I = I_s + I_c = 0$ ).<sup>[21]</sup> The resulting electrical

potential difference that can be measured between the channel ends is the streaming potential ( $(\Delta\varphi_s)_{I=0}$ ).

The total streaming current,  $I_s$ , is obtained by integrating the local streaming current density [product of local electric charge density,  $\rho(r)$ , and local fluid linear velocity,  $v_z(r)$ ] over the channel cross section. For a capillary of radius  $a$ ,  $I_s$  is

$$I_s = \int_0^a 2\pi r v_z(r) \cdot \rho(r) dr \quad (1)$$

The form of the above expression is strictly true only for laminar flow conditions. However, even if the fluid flow is so fast as to be turbulent elsewhere, the expression will hold if the fluid flow is laminar in the thin sublayer near the wall.<sup>[22]</sup>

The distribution of local electric charge density,  $\rho(r)$ , is described by the Poisson equation

$$\frac{d^2\psi}{dr^2} = -\frac{\rho(r)}{\epsilon_0 \epsilon_r} \quad (2)$$

where  $\psi(r)$  is the local electrostatic potential at a distance  $r$  from the axis of the capillary,  $\epsilon_0$  is the vacuum permittivity, and  $\epsilon_r$  is the relative dielectric constant of the solvent.

As shown by Eq. (1), the evaluation of the streaming current also requires a description of the fluid velocity profile. At low flow rates, when the flow is wholly laminar, the velocity profile is given by the classical Hagen-Poiseuille equation (parabolic velocity profile). On the other hand, at high flow rates, the flow becomes turbulent through a core constituting most of the capillary, and in this core the velocity is nearly constant. The flow remains laminar only in a thin sublayer near the walls. The hydrodynamic theory<sup>[23]</sup> gives  $t_{ls}$ , the thickness of this laminar sublayer, as

$$t_{ls} \approx 116a(Re)^{-7/8} \quad (3)$$

where  $Re$  is the Reynolds number, given by

$$Re = \frac{\rho' \bar{v} d_h}{\eta} = \frac{\bar{v} d_h}{\nu} \quad (4)$$

$\bar{v}$  represents the mean velocity of the liquid,  $\rho'$ , its density,  $\eta$ , its dynamic viscosity,  $\nu$ , its kinematic viscosity, and  $d_h$ , the hydraulic diameter.

The laminar sublayer being extremely thin (in comparison with the diameter of the capillary), one can consider that the velocity gradient is constant

inside this layer. If the EDL lies within this laminar sublayer, the velocity  $v_z$  at any distance  $w$  ( $w = a - r$ ) from the wall is given by<sup>[23]</sup>

$$v_z(w) = \int_0^w \left( \frac{dv}{dw} \right)_{w=0} dw \approx \int_0^w \frac{v_f^2}{\nu} dw = \frac{v_f^2}{\nu} w \quad (5)$$

with  $v_f$ , the friction velocity, which takes the following form:

$$v_f = \sqrt{\frac{a\Delta P}{2\rho l}} \quad (6)$$

$\Delta P$  represents the hydrostatic pressure drop through the capillary and  $l$ , its length.

One can remark that the velocity gradient in the laminar sublayer during turbulent flow is much higher than that during wholly laminar flow, since most of the velocity gradient occurs in this region.

Inserting Eq. (2) (after substituting  $r = a - w$ ) and (5) into Eq. (1) and integrating by parts gives the approximate relation:

$$I_s \approx \frac{2\pi\epsilon_0\epsilon_r v_f^2}{\nu} \left[ \left( w \cdot (a - w) \cdot \frac{d\psi}{dw} \right)_{w=a}^{w=0} - \int_a^0 \frac{d\psi}{dw} \cdot (a - 2w) dw \right] \quad (7)$$

Since  $d\psi/dw = 0$  and  $\psi = 0$  when  $w = a$  (the radius of the capillary being much greater than the thickness of the EDL), and since also  $\psi = \zeta$  when  $w = 0$ , this reduces to

$$I_s \approx -\frac{\pi\epsilon_0\epsilon_r a^2 \Delta P \zeta}{\eta l} \quad (8)$$

This relation should apply when the flow is turbulent, provided that  $t_{ls} > \kappa^{-1}$ , the Debye length.

As mentioned earlier, the flow-induced streaming potential produces a conduction current ( $I_c$ ) that just balances the streaming current ( $I_c = -I_s$ ) and depends on the electric resistance (or its inverse the electric conductance) presented by the system substrate/channel. By applying Ohm's law ( $\Delta\varphi_s = I_c/G_t$ ) and using Eq. (8), the relation between the  $\zeta$ -potential and the streaming potential coefficient is obtained:

$$\zeta = \frac{l\eta G_t}{\pi a^2 \epsilon_0 \epsilon_r} \left( \frac{\Delta\varphi_s}{\Delta P} \right)_{l=0} \quad (9)$$

where  $G_t$  denotes the overall electric conductance of the system.

The right-hand-side of this equation contains measurable values ( $\Delta\varphi_s/\Delta P$  and  $G_t$ ), characteristics of channel geometry ( $l$  and  $a$ ), which are usually available for well-defined channels and reasonably known values ( $\eta$  and  $\epsilon_r$ ).

Unlike the streaming current, which has a convective nature and occurs only where the macroscopic liquid flow is possible (i.e., inside the channel), the conduction current flows wherever the electric conductivity is nonzero.<sup>[20]</sup> So, in the case of channels whose walls are formed by a conducting material such as a porous membrane soaked with electrolyte solution, the conduction current can flow through two paths (Fig. 1): the channel and the membrane pores. Both of them can contribute to the conduction process either by a bulk conductivity ( $\lambda_0$ ) or by a higher conductivity resulting from a non-negligible surface conductance contribution of the channel walls and/or the membrane pore walls.

The overall electric conductance of the system,  $G_t$ , is the sum of the channel conductance,  $G_c$ , and the membrane conductance,  $G_m$ . In the case of large channels (electrokinetic radius  $a/\kappa^{-1} \gg 1$ ), the surface conductance of the channel walls ( $G_s$ ) provides a negligible part of the channel conductance, which is given by

$$G_c = \left( \lambda_0 + \frac{2G_s}{a} \right) \cdot \frac{\pi a^2}{l} \quad (10)$$

and can be omitted. The channel conductance can then be written as

$$G_c = \frac{\lambda_0 \pi a^2}{l} \quad (11)$$

In addition, if the material forming the channel walls is nonconducting or provides a negligible part of the overall electric conductance, then  $G_t = G_c = (\lambda_0 \pi a^2)/l$ .

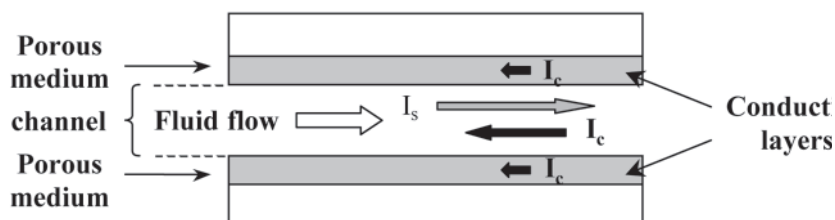


**Figure 1.** Schematic representation of the different paths for the streaming and conduction currents. Steady state:  $I = I_s + I_c = 0$ .

In these conditions ( $G_s$  and  $G_m$  are negligible or zero), Eq. (9) becomes the classical Helmholtz-Smoluchowski equation:

$$\zeta = \frac{\eta \lambda_0}{\epsilon_0 \epsilon_r} \left( \frac{\Delta \varphi_s}{\Delta P} \right)_{l=0} \quad (12)$$

Finally, it should be mentioned that for turbulent flow ( $Re > \sim 2000$ ), the volume flow rate of liquid in a channel does not vary linearly with the pressure unlike laminar flow conditions. In the case of the smooth wall, the volume flow rate takes the following form:<sup>[24]</sup>

$$u = \pi a^2 v_f \left( 2.5 \ln \left( \frac{av_f}{v} \right) + 2.04 \right) \quad (13)$$

### 3. EXPERIMENTAL

#### 3.1 Membrane and Chemicals

The membrane tested in this study is a ceramic membrane manufactured by TAMI Industry (Nyons, France). It has a multilayer structure with a titania filtering layer (MWCO of 1500 Da) which is  $\sim 1.6 \mu\text{m}$  in thickness<sup>[25]</sup> and a tubular shape of 10 mm in external diameter and 600 mm in length, composed of three identical channels in clover with a hydraulic diameter of 3.6 mm and a wetted perimeter of 12.22 mm/channel (Clover CéRAM INSIDE<sup>®</sup>) (Fig. 2).

As can be seen in Fig. 2, the shape of the cross section of a channel is not strictly circular. However, it may be approximated as circular with a radius of

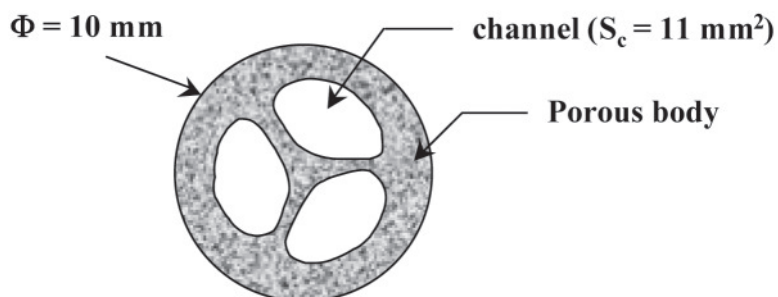


**Figure 2.** Cross-section view of the tubular membrane (Clover CéRAM INSIDE<sup>®</sup>). Hydraulic diameter and wetted perimeter for a channel: 3.6 mm and 12.2 mm, respectively.

1.87 mm, giving a cross-section area of 11 mm<sup>2</sup> (which is obviously strictly identical to the cross-section area of a channel) and a wetted perimeter of 11.75 mm (value very close to 12.22 mm).

A characterization of the membrane in terms of hydraulic permeability, salts, and neutral solutes rejection (measured at different salt concentrations and pH values) can be found in.<sup>[25]</sup>

Tangential streaming potential measurements were performed in 10<sup>-3</sup> M KCl solutions at various pH ranging from 3.5 to 10.0. This concentration value was chosen to obtain streaming potentials high enough. Electrolyte solutions were prepared from potassium chloride of pure analytical grade and milli-Q quality water (conductivity < 1  $\mu$ S cm<sup>-1</sup>). The pH was adjusted by addition of 0.1 M HCl and KOH solutions.

### 3.2 Electrokinetic Setup for the Characterization of Tubular Membranes

The in-house-built device used in this work is depicted in Figs. 3a and b. It consists of a polycarbonate tubular module of 720 mm in length, inside which the tubular membrane is inserted.

From a feed container (volume = 10 L), a Tuthill volumetric pump (at variable flow rate) allows circulation of the solution to the membrane module where it flows inside channels over the filtering layer of the membrane. During the streaming potential measurement, the retentate stream must not be recycled so as to avoid a possible short. It is collected in another container. The pressure drop along the membrane induced by the circulation of the liquid through the channels is regulated by the feed flow rate. It is measured by a differential pressure transducer (Mesurex). A pressure loss until 100 mbar can be obtained with this pump and the membrane under consideration. The membrane module is also equipped with two Ag/AgCl wire electrodes, placed on each side from channels (just at the inlet and outlet of channels), and linked to a Tacussel multimeter (model Minisis 20000) to measure the streaming potential ( $\Delta\varphi_s$ ) developed in the solution along the membrane.

For conductance measurements, two cylindrical cells of 10 mm in length are screwed on each side from the membrane module (Fig. 3b). Each cell is equipped with a disk-shaped Ag/AgCl electrode (3.6 cm in diameter) fixed at the external side of the cell. Conductance measurements are performed by using the galvanostatic four-electrode mode: the disk Ag/AgCl electrodes are used to inject the current whereas the two Ag/AgCl wires permit to measure the resulting voltage. The equipment used is an electrochemical

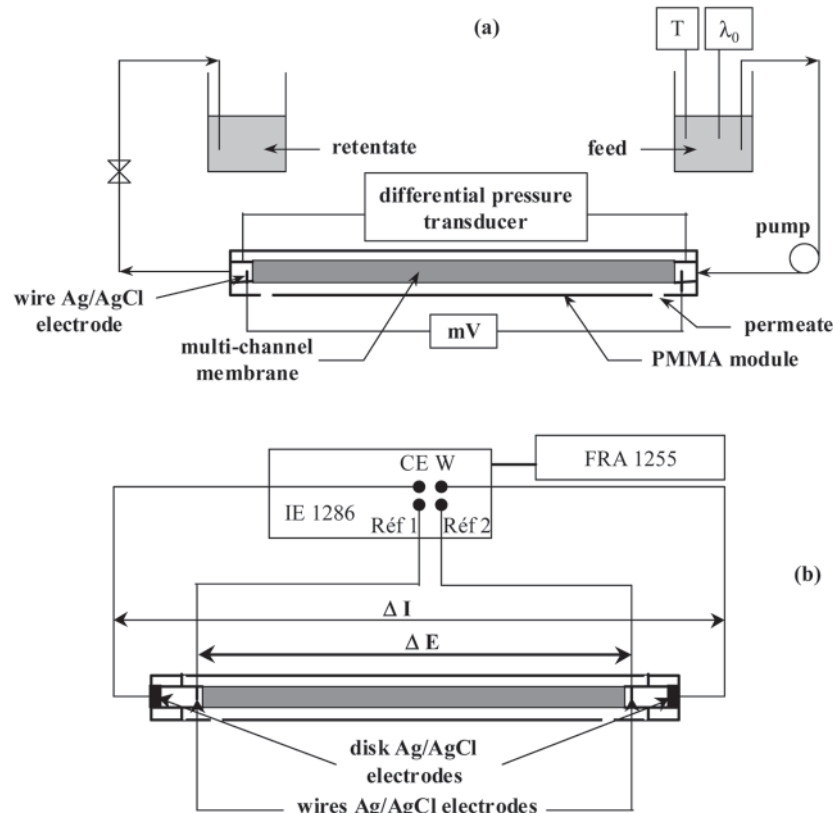


**Figure 3.** Experimental setup (a) for tangential streaming potential measurements; (b) for conductance measurements.

impedance spectrometer (composed of a Solartron 1286 electrochemical interface linked to a Solartron 1255 frequency response analyzer).

The electrodes are made by anodic deposition of silver chloride on silver wires and plates in a 0.1 M HCl solution at a current density of  $0.5 \text{ mA cm}^{-2}$  for  $\sim 30 \text{ min}$ .

Tangential streaming potential and electrical conductance measurements were carried out according to the following procedure. The measuring solution is first forced through pores of the membrane by applying a pressure difference (between retentate and permeate sides) of  $\sim 0.5 \text{ bar}$  so as to equilibrate the membrane with the measuring solution. The pressure difference value can be adjusted by means of a valve located at the retentate circuit outlet. Both retentate and permeate were continuously recycled and their pH as well as

their conductivity were regularly checked. The tangential streaming potential experiments were performed when both pH and conductivity reached almost constant values. The streaming potential ( $\Delta\varphi_s$ ) was measured for continuously increasing pressure values. The streaming potential coefficient was then determined from the slope of the plot of  $\Delta\varphi_s$  vs.  $\Delta P$ . The temperature of the solution was also checked during tangential streaming potential measurements ( $20 \pm 2^\circ\text{C}$ ).

The measurement of the tangential streaming potential was always followed by the electrical conductance measurement before changing the solution (other pH value). The conductance measurement was repeated three to four times, the two cylindrical cells (at the ends of the membrane module) being removed from and then re-screwed on the membrane module before each new measurement. Electrical conductance measurements were carried out in the absence of liquid flow with frequencies ranging from  $10^5$  to  $10^{-1}$  Hz in order to determine the “true” value of the resistance (and not the real part of an impedance).

### 3.3 Hydrodynamic Characterization

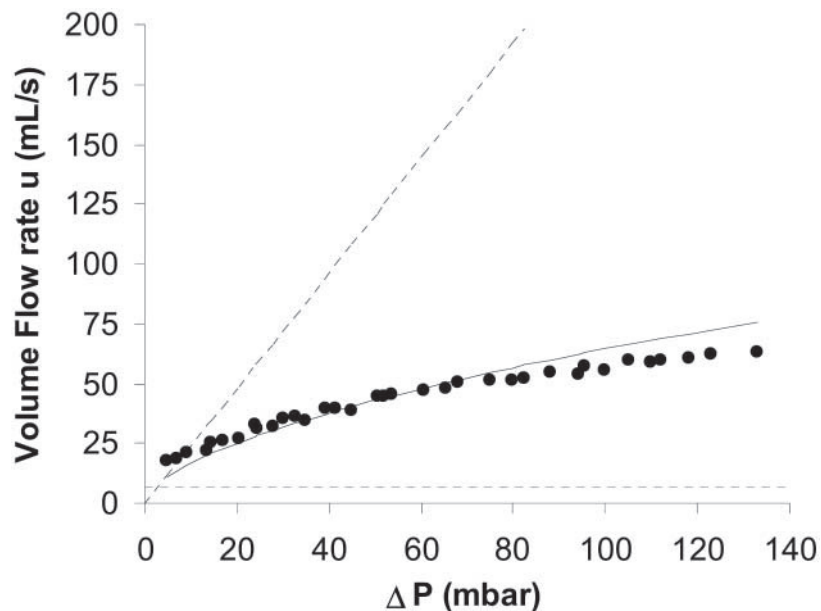
The Reynolds number  $\text{Re}$  [Eq. (3)] is used to describe the flow state in the channels. Volume flow rates of 20 to  $60 \text{ mL}\cdot\text{s}^{-1}$  (measured for pressure values comprised between 5 and  $\sim 120$  mbar) translate to mean velocities  $\bar{v}$  of 0.606 to  $1.818 \text{ m}\cdot\text{s}^{-1}$ , giving  $\text{Re} = 2182\text{--}6546$ . Thus, the flow can be regarded as turbulent for the pressure range studied. It should be mentioned that turbulent flow is established in a short distance of  $\sim 20$  mm (given by  $0.63 \cdot d_h \cdot \text{Re}^{0.25}$ ) from the membrane inlet.<sup>[24]</sup>

Figure 4 gives an example of the volume flow-rate variation as a function of pressure drop along the tube (symbols). As can be seen, the flow rate is not a linear function of  $\Delta P$  (the Hagen-Poiseuille relation fails to describe experimental results as shown by the dotted line), which is in accordance with the Reynolds number ( $\text{Re} > \sim 2000$ ). The experimental data are fairly described by Eq. (13), which holds for turbulent flow in the case of smooth walls (full line).

When  $\bar{v} = 60 \text{ mL}\cdot\text{s}^{-1}$ , the purely laminar sublayer extends to  $\sim 100 \mu\text{m}$  from the channel. Thus, the EDL whose thickness is  $\sim 10 \text{ nm}$  is within this laminar sublayer. Consequently, Eqs. (9) and (12) can be used to calculate  $\zeta$ -potential.

## 4. RESULTS AND DISCUSSION

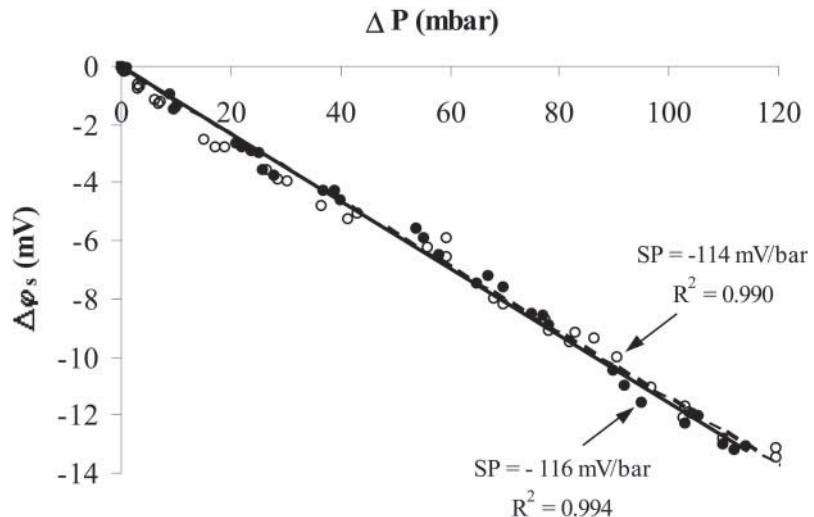
A first preliminary study allowed investigation of the effect of pressure and fluid permeation through the membrane pores on the measured streaming potential.



**Figure 4.** Volume flow rate ( $u$ ) as a function of pressure difference ( $\Delta P$ ). (●): experimental data obtained in  $10^{-3}$  M KCl solution; pH = 10.0. Dotted line: Hagen-Poiseuille relation ( $u = \pi a^4 \Delta P / 8\eta l$ ). Full line: turbulent flow in the case of smooth walls [Eq. (13)].

Figure 5 shows the variation of the streaming potential as a function of the applied pressure difference for a  $10^{-3}$  M KCl solution at pH = 10.0. As expected, the streaming potential difference varies linearly vs. the applied pressure although the flow is not wholly laminar. The electrokinetics theory therefore remains valid if the EDL lies inside a laminar layer near the wall even if the flow is so fast as to be turbulent elsewhere. The streaming potential is obtained from the slope of  $\Delta\varphi_s = f(\Delta P)$ , which is constant in the pressure range 0–120 mbar.

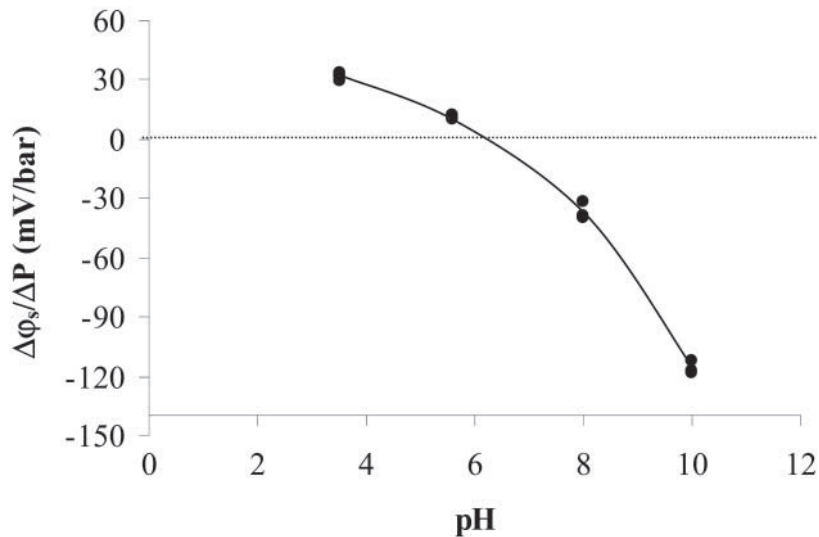
In order to ensure that the fluid permeation through the membrane pores does not influence tangential streaming potential measurements (performed by flow across the top surface of the membrane), we have also performed these measurements on a membrane coated by a PTFE film on its external surface in order to avoid any permeation. The results obtained show that there is no significant effect of the permeation of the liquid through the membrane on the tangential streaming potential measurements (Fig. 5). Indeed, the  $\zeta$ -potential values obtained with and without PTFE film are very close:  $-116$  mV and  $-114$  mV, respectively.



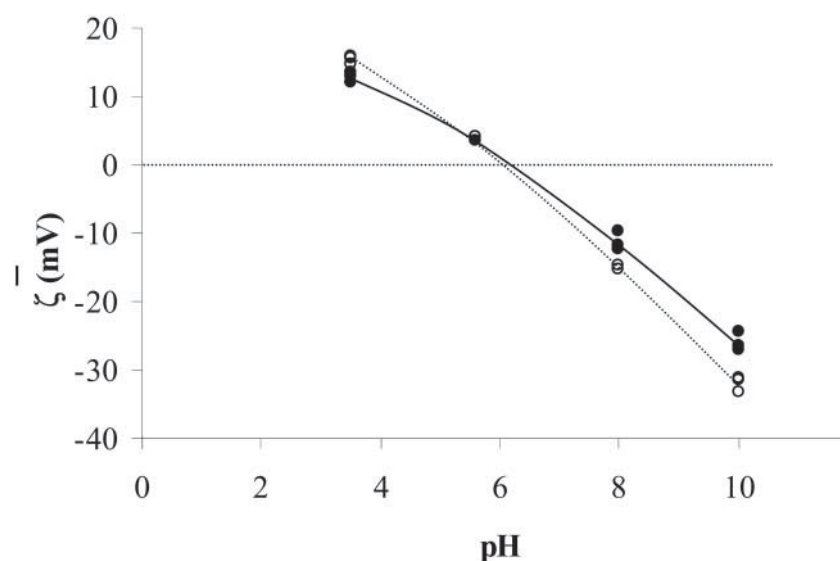
**Figure 5.** Streaming potential ( $\Delta\varphi_s$ ) as a function of pressure difference ( $\Delta P$ ) in a 0.001 M KCl solution; pH = 10.0. (●): membrane coated by a PTFE film on its external surface. (○): bare membrane.

Figure 6 presents the pH dependence of streaming potential coefficient ( $\Delta\varphi_s/\Delta P$ ) for a  $10^{-3}$  M KCl solution. The sign of the streaming potential directly yields the sign of the net charge of the membrane, i.e., the global charge behind the shear plane. The curve shape is typical of the amphoteric behavior of metal oxides and results from the shifting of the proton equilibrium that occurs at the surface when pH moves. The isoelectric point (iep), i.e., the particular pH for which the net charge on the membrane surface (and so, the streaming potential) is zero, is found to be close to 6.1. This value is in good agreement with that obtained from KCl retention data ( $\sim 6.2$ , see ref.<sup>[25]</sup>). This result confirms the reliability of the new tangential streaming potential setup for the electrokinetic characterization of tubular membranes.

$\zeta$ -potential values were determined in two ways: (i) from the streaming potential data only by means of the classical Helmholtz-Smoluchowski equation [Eq. (9)], which neglects membrane body conductance ( $G_m$ ) and surface conductance of the channel ( $G_s$ ) and (ii) from coupled measurements of streaming potential and electric conductance by means of Eq. (12) (accounting for membrane body conductance,  $G_m$ ). Results are presented in Fig. 7.



**Figure 6.** pH-dependence of streaming potential coefficient ( $\Delta\varphi_s/\Delta P$ ) in a 0.001 M KCl solution.



**Figure 7.** pH-dependence of  $\zeta$ -potential in a 0.001 M KCl solution; (○): correct  $\zeta$ -potential determined from streaming potential and electrical conductance [Eq. (9)]; (●): apparent  $\zeta$ -potential calculated from Helmholtz-Smoluchowski relationship [Eq. (12)].

It first appears that the  $\zeta$ -potential values calculated by means of the Helmholtz-Smoluchowski equation are lower in the whole range of pH under consideration. This underestimation of  $\zeta$ -potential results from the negligence of the conduction phenomenon through the membrane pores. Indeed, the contribution of the channel walls' surface conductivity ( $G_s \cdot P_w/S_c$ ) to the channel conductivity cannot be invoked for so large a channel size (the ratio of the radius to the Debye length,  $a/\kappa^{-1}$ , being of  $\sim 1.9 \times 10^5$ ). Nevertheless, the discrepancy between  $\zeta$  values determined with and without membrane porous body conductivity correction remains low and does not exceed 22% (Fig. 8).

Furthermore, the  $(\zeta - \zeta_{HS})/\zeta$  ratio does not seem to be influenced by pH (a mean value of  $\sim 17\%$  is obtained). This behavior indicates that the pore walls' surface conductivity is a negligible contribution of the conductivity within membrane pores. Indeed, the porous structure acts on the tangential streaming potential process only by its bulk conductivity and that is why a virtually constant  $(\zeta - \zeta_{HS})/\zeta$  ratio is obtained, whatever the pH. On the other hand, if the pore wall surface conductance was not negligible, the  $(\zeta - \zeta_{HS})/\zeta$  ratio would be dependent of pH and would increase as pH moves away from the iep resulting from the increase in pore wall surface

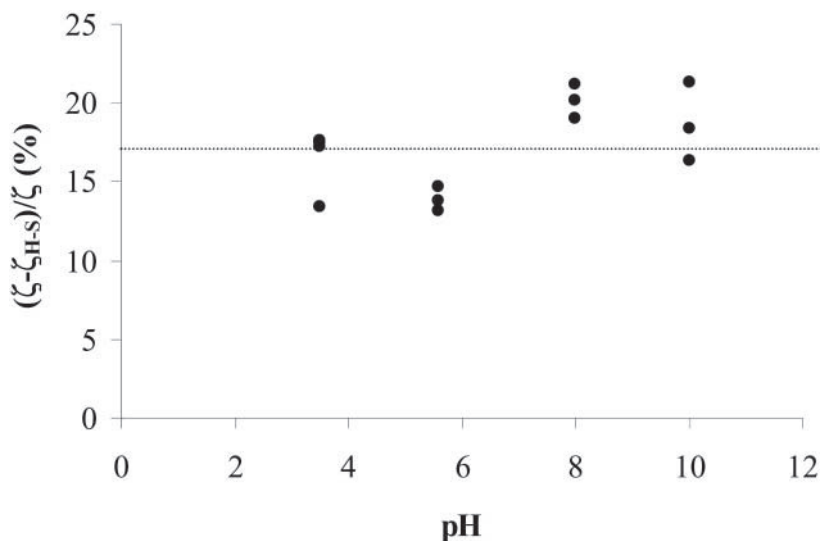


**Figure 8.** pH-dependence of the parameter  $(\zeta - \zeta_{HS})/\zeta$  in a 0.001 M KCl solution;  $\zeta$ : correct  $\zeta$ -potential determined from streaming potential and electrical conductance [Eq. (9)];  $\zeta_{HS}$ : apparent  $\zeta$ -potential calculated from Helmholtz-Smoluchowski relationship [Eq. (12)].

conductance as the electrical charge becomes higher (due to exponential rise of counterion concentration within EDL).

It should also be noted that the correct  $\zeta$ -potential value determined at pH = 3.5 (15.4 mV) is in good agreement with that obtained by the tangential streaming potential method applied to a flat membrane made of the same material: 11.4 mV.<sup>[19]</sup> In this case, measurements were carried out using a parallel-plate channel of a rectangular cross section formed by clamping together two identical plane membranes separated by a PTFE spacer. This result is a further validation of our experimental method. It has the advantage that it only requires two measurements (streaming potential and electrical conductance) to evaluate the correct  $\zeta$ -potential unlike the traditional microslit electrokinetic setup that needs many tangential streaming potential measurements at various spacer thicknesses. This latter procedure is rather tedious and not feasible for nonflat solid specimens anyway.

## 5. CONCLUSION

A home-made tangential streaming potential setup for the electrokinetic characterization of tubular membranes was described and tested. This method consists in forcing the liquid through the channels of the membrane where it flows over the filtering layer of this latter and measuring the resulting electrical potential difference between the inlet and outlet of the tube. The work was focused on the electrokinetic characterization of a low-ultrafiltration CéRAM INSIDE® ceramic membrane.

The setup was validated by:

- The good linear regression of the plot  $\Delta\varphi_s = f(\Delta P)$ .
- The iep value that is in very good agreement with that obtained from salt retention data.
- The  $\zeta$ -potential value determined at pH = 3.5 that is very close to that obtained on a flat membrane made of the same material using the traditional microslit tangential streaming potential set-up.

Although the flow was not wholly laminar (because of the large hydraulic diameter of channels), the electrokinetics theory could be used to convert the streaming potential data into  $\zeta$ -potentials because the EDL lay within a laminar sublayer near the channel walls. Streaming potential coupled with electrical conductance measurements allowed to evaluate the correct  $\zeta$ -potential by accounting for the conduction through the membrane pores filled with electrolyte solution. It was shown that neglecting the conduction phenomenon inside the porous body leads to a low underestimation of the

$\zeta$ -potential (less than  $\sim 20\%$ ). This low discrepancy between the correct  $\zeta$ -potential ( $\zeta$ ) and the apparent one (deduced from the classical Helmholtz-Smoluchowski formula,  $\zeta_{H-S}$ ) can be explained by the large size of channels in comparison with the membrane porous body.

It should be mentioned that most of commercial tubular membranes are composed of macrochannels and therefore the single measurement of the streaming potential allows us to evaluate satisfactorily the  $\zeta$ -potential of the membrane surface.

The results also show that the ratio  $\zeta/\zeta_{H-S}$  is independent of pH here. This suggests that the surface conductivity of the pore walls constitutes only a negligible share of the overall conductivity within membrane pores, i.e., the porous body acts on the tangential streaming potential process only by its bulk conductivity.

Finally, a major advantage of this new method is that it also allows assessing the  $\zeta$ -potential of tubular membranes composed of channels of arbitrary size and shape.

## LIST OF SYMBOLS

### Roman Letters

a	Capillary radius (m)
$d_H$	Hydraulic diameter (m)
$G_c$	Channel conductance ( $\Omega^{-1}$ )
$G_m$	Membrane conductance or porous body conductance ( $\Omega^{-1}$ )
$G_s$	Surface conductance of the pore walls ( $\Omega^{-1}$ )
$G_t$	Total conductance of the membrane porous body/channel(s) system ( $\Omega^{-1}$ )
I	Electric current (A)
$I_c$	Conduction current (A)
$I_s$	Streaming current (A)
$l$	Channel length (m)
P	Hydrostatic pressure ( $N \cdot m^{-2}$ )
$P_w$	Wetted perimeter of a channel (m)
Re	Reynolds number (-)
r	Distance from the axis of the capillary (m)
$S_c$	Cross-sectional area of channel(s) ( $m^2$ )
$t_{ls}$	Thickness of laminar sublayer (m)
u	Volume flow rate ( $m^3 \cdot s^{-1}$ )
v	Fluid velocity ( $m \cdot s^{-1}$ )
$\bar{v}$	Mean velocity of the fluid ( $m \cdot s^{-1}$ )
$v_f$	Friction velocity ( $m \cdot s^{-1}$ )

$z$	Axial coordinate (m)
$w$	Distance from the channel wall (m)

### Greek Letters

$\epsilon_0$	Vaccum permittivity ( $8.854 \times 10^{-12} \text{ F} \cdot \text{m}^{-1}$ )
$\epsilon_r$	Relative dielectric constant of the solvent
$\lambda_0$	Conductivity of bulk electrolyte ( $\Omega^{-1} \cdot \text{m}^{-1}$ )
$\Phi$	Diameter of the tubular membrane (m)
$\kappa^{-1}$	Debye length (-)
$\rho$	Electric charge density ( $\text{C} \cdot \text{m}^{-3}$ )
$\rho'$	Density ( $\text{kg} \cdot \text{m}^{-3}$ )
$\eta$	Dynamic viscosity of the electrolyte ( $\text{kg} \cdot \text{m}^{-1} \cdot \text{s}^{-1}$ )
$\nu$	Kinematic viscosity of the electrolyte (=dynamic viscosity/density) ( $\text{m}^2 \cdot \text{s}^{-1}$ )
$\varphi$	Electrical potential (V)
$\psi$	Electrostatic potential (V)
$\zeta$	Zeta potential (V)

### REFERENCES

1. Nyström, M.; Lindström, M.; Matthiasson, E. Streaming potential as a tool in the characterization of ultrafiltration membranes. *Colloid Surf.* **1989**, *36*, 297–312.
2. Staude, E.; Duputell, D.; Malejka, F.; Wyszynski, D. Determination of surface properties of membranes based on polysulfone derivatives by electrokinetic measurements. *J. Disp. Sci. Technol.* **1991**, *12*, 113–127.
3. Werner, C.; Jacobasch, H.J.; Reichelt, G. Surface characterization of hemodialysis membranes based on streaming potential measurements. *J. Biomater. Sci.* **1995**, *7*, 61–76.
4. Kim, K.J.; Fane, A.G.; Nyström, M.; Pihlajamaki, A.; Bowen, W.R.; Mukhtar, H. Evaluation of electroosmosis and streaming potential for measurement of electric charges of polymeric membranes. *J. Membr. Sci.* **1996**, *116*, 149–159.
5. Szymczyk, A.; Pierre, A.; Reggiani, J.C.; Pagetti, J. Characterisation of the electrokinetic properties of plane inorganic membranes using streaming potential measurements. *J. Membr. Sci.* **1997**, *134*, 59–66.
6. Ricq, L.; Szymczyk, A.; Fievet, P. Electrokinetic methods employed in the characterization of microfiltration and ultrafiltration membranes. In *Interfacial Electrokinetics and Electrophoresis*; Marcel Dekker Inc; 2002; Chap. 20, 583–617.

7. Lettmann, C.; Mockel, D.; Staude, E. Permeation and tangential flow streaming potential measurements for electrokinetic characterization of track-etched microfiltration membranes. *J. Membr. Sci.* **1999**, *145*, 243–251.
8. Van Wagenen, R.A.; Andrade, J.D. Flat plate streaming potential investigations: hydrodynamics and electrokinetic equivalency. *J. Colloid Interf. Sci.* **1980**, *76*, 305–314.
9. Jacobasch, H.J.; Schurz, J. Characterization of polymer surfaces by means of electrokinetic measurements. *Prog. Colloid Polym. Sci.* **1988**, *77*, 40–48.
10. Möckel, D.; Staude, E.; Dal-Cin, M.; Darcovich, K.; Guiver, M. Tangential flow streaming potential measurements: hydrodynamic cell characterization and zeta potentials of carboxylated polysulfone membranes. *J. Membr. Sci.* **1998**, *145*, 211–222.
11. Erickson, D.; Li, D.; Werner, C. An improved method of determining the  $\zeta$ -potential and surface conductance. *J. Colloid Interf. Sci.* **2000**, *232*, 186–197.
12. Zembala, M.; Adamczyk, Z. Measurements of streaming potential for mica covered by colloid particles. *Langmuir* **2000**, *16*, 1593–1601.
13. Werner, C.; Körber, H.; Zimmerman, R.; Dukhin, S.; Jacobasch, H.J. Extended electrokinetic characterization of flat solid surfaces. *J. Colloid Interf. Sci.* **1998**, *208*, 329–346.
14. Szymczyk, A.; Fievet, P.; Reggiani, J.C.; Pagetti, J. Characterisation of surface properties of ceramic membranes by streaming and membrane potentials. *Desalination* **1998**, *116*, 81–88.
15. Szymczyk, A.; Labbez, C.; Fievet, P.; Aoubiza, B.; Simon, C. Streaming potential through multilayer membranes. *AIChE* **2001**, *47*, 2349–2358.
16. Benavente, J.; Jonsson, G. Electrokinetic characterization of composite membranes: estimation of different electrical contributions in pressure induced potential measured across reverse osmosis membranes. *J. Membr. Sci.* **2000**, *172*, 189–197.
17. Canas, A.; Ariza, M.J.; Benavente, J. Characterization of active and porous sublayers of a composite reverse osmosis membrane by impedance spectroscopy, streaming potential and membrane potentials, salt diffusion and X-ray photoelectron spectroscopy measurements. *J. Membr. Sci.* **2001**, *183*, 135–146.
18. Yaroshchuk, A.E.; Boiko, Y.P.; Makovetskiy, A.L. Filtration potential across membranes containing selective layers. *Langmuir* **2002**, *18* (10), 5154–5162.
19. Fievet, P.; Sbaï, M.; Szymczyk, A.; Vidonne, A. Determining the  $\zeta$  potential of plane membranes from tangential streaming potential measurements: effect of the membrane body conductance. *J. Membr. Sci.* **2003**, *226*, 227–236.

20. Yaroshchuk, A.E.; Ribitsch, V. Role of channel wall conductance in the determination of  $\zeta$ -potential from electrokinetic measurements. *Langmuir* **2002**, *18*, 2036–2038.
21. Hunter, R.J. *Zeta Potential in Colloid Science, Principles and Applications*. Academic Press: San Diego, 1981.
22. Holstein, W.L.; Hayes, L.J.; Robinson, E.M.C.; Laurence, G.S.; Buntine, M.A. Aspects of electrokinetic charging in Liquid Microjets. *J. Phys. Chem. B* **1999**, *103*, 3035–3042.
23. Joulié, R. *Mécanique des Fluides Appliquées, Ch. VIII: Ecoulement dans les conduites cylindriques*; 1998; 176, Ellipses.
24. Padet, J. *Fluides en Écoulement, Ch. VI: Ecoulements internes*; 1991; 274, Masson.
25. Labbez, C.; Fievet, P.; Szymczyk, A.; Vidonne, A.; Foissy, A.; Pagetti, J. Analysis of the salt retention of a titania membrane using the DSPM model: effect of pH, salt concentration and nature. *J. Membr. Sci.* **2002**, *208*, 315–329.

Received March 2, 2004

Accepted June 13, 2004